ACADEMIA ROMÂNĂ
Revue Roumaine de Chimie
http://web.icf.ro/rrch/

Rev. Roum. Chim.,
2018, *63*(10), 873-880

ELECTRONIC AND OPTICAL PROPERTIES OF TiS_2 DETERMINED FROM MODIFIED BECKE–JOHNSON GGA POTENTIAL (mBJ-GGA) STUDY

Hamza EL-KOUCH and Larbi EL FARH*

Mechanics and Energetic Laboratory, Faculty of Sciences, University Mohammed 1st, Oujda, Morocco

Received May 2, 2017

In this study, we report the results of electronic structure and optical properties of TiS_2 calculations within the density functional theory (DFT) using the generalized gradient approximation (GGA) and an improved version of the modified Becke-Johnson (mBJ) exchange-correlation potential. The equilibrium lattice parameters and bulk modulus were found to be close to the experimentally reported results and a semi-conducting character of the material was revealed from the band structure calculation with an indirect band gap of 0.26 eV. Furthermore, DOS plots showed a prominent contribution of Ti-d, S-s and S-p. We have also calculated the dielectric function, refractive index and optical reflectivity and we have compared the obtained curves to those found experimentally by other authors.

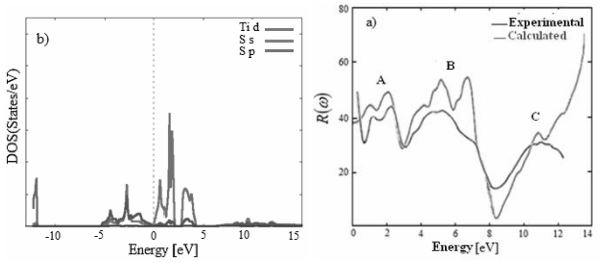

INTRODUCTION

Recent progress in material sciences has shown that the dimensionality of materials plays a crucial role in determining their fundamental properties.[1] Especially, the two-dimensional materials, like the graphene, have shown rich physical properties not observed in bulk or in the one-dimensional materials. For this reason, in the latest years the properties of other 2D materials like transition-metal dichalcogenides (TMDs) have known a renewal of interest due to their potential applications in next-generation nanoelectronic devices.[2] The titanium disulfide (TiS_2) is one of those materials; it consists of covalently bonded Ti and S atoms arranged in two-dimensional hexagonal planes.[3] The layers are stacked together by weak Van Der Waals forces.[4] TiS_2 has been widely studied in recent years because of its use in numerous applications, particularly as a cathode material in rechargeable batteries,[5] as hydrogen storage material,[6] and as a high-performance thermoelectric material.[7] In literature, there are many conflicting results on the electronic structure of TiS_2, since it is still debated whether the material is metallic, semi-metallic or semiconductor.[8-12] Several experimental works have reported that TiS_2 has semiconductor behavior with a band gap ranging from 0.05 to 2.5 eV.[8-10] At the same time, other works classify TiS_2 among metals[11] or semi-metals[12] with an indirect band gap overlap (between the points Γ and L in the first Brillouin zone).

The aim of the present paper is to investigate the electronic, structural and optical properties of TiS_2 using density functional theory (DFT) and full potential linearized and augmented plane wave (FLAPW) basis set.

COMPUTATIONAL METHODS

The calculations presented in this paper have been performed within the framework of density functional theory (DFT) using the full-potential linearized augmented plane wave (FP-LAPW)

* Corresponding author: l.elfarh@ump.ac.ma; Phone: +212628378953.

method[13] as implemented in the Wien2K code.[14] The mBJ potential for the exchange correlation potential[15] was used to calculate electronic and optical properties.

The modified Becke-Johnson potential (mBJ) as proposed by Tran and Blaha[16] is:

$$V_{X,\sigma}^{mBJ}(r) = CV_{X,\sigma}^{BR} + (3C-2)\frac{1}{\pi}\sqrt{\frac{5}{12}}\sqrt{\frac{2t_\sigma(r)}{\rho_\sigma(r)}} \quad (1)$$

where C is a system-dependent parameter, with C = 1 corresponding to the original BJ potential, $\rho_\sigma = \sum_{i=1}^{N_\sigma}|\psi_{i,\sigma}|^2$ is the electronic density, $t_\sigma = \left(\frac{1}{2}\right)\sum_{i=1}^{N_\sigma}\nabla\psi_{i,\sigma}^{*}\nabla\psi_{i,\sigma}$ is the kinetic energy density and $V_{X,\sigma}^{BR}(r)$ is the Becke-Roussel (BR) potential[17] given by:

$$V_{X,\sigma}^{BR}(r) = -\frac{1}{b_\sigma(r)}\left(1 - e^{-X_\sigma(r)} - \frac{1}{2}X_\sigma(r)e^{-X_\sigma(r)}\right) \quad (2)$$

$V_{X,\sigma}^{BR}(r)$ was originally proposed to mimic the Slater potential, the Coulomb potential corresponding to the exact exchange hole.

X_σ is determined from an equation involving ρ_σ, $\nabla\rho_\sigma$, $\nabla^2\rho_\sigma$ and t_σ.

b_σ is calculated by: $b_\sigma = \left[\frac{X_\sigma^3 e^{-X_\sigma}}{8\pi\rho_\sigma}\right]^{\frac{1}{3}}$.

In eq. (1), parameter C was proposed by Tran and Blaha[16], for bulk crystalline materials, by the following empirical relation:

$$C = -0.012 + 1.023\left(\frac{1}{V_{cell}}\int_{cell}\frac{|\nabla\rho(r')|}{\rho(r')}d^3r'\right)^{\frac{1}{2}} \quad (3)$$

where V_{cell} is the volume of the unit cell.

Larger C values than 1 lead to a less negative (less attractive) potential, in particular, in low-density regions.

In the FP-LAPW method, a unit cell is divided into an interstitial zone and non-interweaving spheres known as muffin-tin (MT) of a specific radius (RMT). Inside the MT spheres, the basis sets are described by a linear combination of radial solutions of Schrödinger equation (for a single particle and at fixed energy) along with the energy derivatives time spherical harmonics. Inside each MT sphere, the set of basis is divided into subsets (core and valence). The spherically symmetric charge density core subsets are completely confined inside the MT sphere. The muffin-tin radii RMT were chosen equal to 2.34 for Ti and 2.08 Å for S. The R_{MT}*$Kmax$ parameter was taken equal to 9. To ensure the correctness of our calculations, we have taken l_{max} = 10 and G_{max} = 12. Also, in the self-consistent calculations, we consider that the total energy is converged to within 0.1 mRy. Note that we have used 900 K-points in the first Brillouin zone for k-space integration to achieve self-consistency.

RESULTS AND DISCUSSION

1. Structural Properties

The titanium disulfide TiS_2 has a layered hexagonal structure with space group P-3m1 (No. 164).[15] One Ti atom is located at 1a (0, 0, 0) and two S atoms at 2d (1/3, 2/3, 1/4) and (2/3, 1/3, 3/4) in the unit cell, as shown in Figure 1.

The lattice parameters and all atomic positions within a crystal unit cell have been relaxed in order to reach equilibrium configuration. The relaxation was performed simulating the XC effects by generalized gradient approximation (GGA) with Perdew, Burke and Ernzerhof (PBE) parameterization. Electronic structure and optical calculations were then performed on this, fully relaxed structure simulating the XC effects by modified Becke-Johnson. This choice has been made due to that it has been demonstrated[16] that the mBJ provides a better description of the band gaps and optical properties.

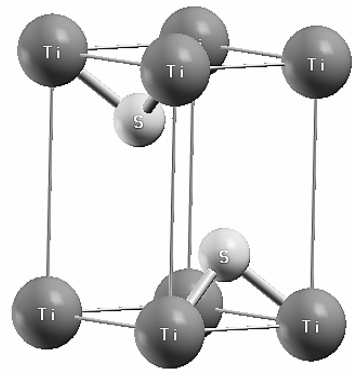

Fig. 1 – Unit cell of TiS_2.

Table 1

Structural parameters derived from Murnaghan-Birch equation of state

	a (Å)	*b (Å)*	*c (Å)*	$V_0[Å^3]$	$B_0[GPa]$	B_0'	$E_0[Ry]$
Present work	3.31	3.31	5.55	59.10	95.6281	4.2432	-3304.704936
Experiment	3.407[18]	3.407[18]	5.695[18]	57.24[4]	45.90[4]	9.50[4]	
Other works				51.72[4]	58.91[4]	4.11[4]	

In the present work the TiS_2 structure was fully optimized, *i.e.* the lattice parameters and all the atomic positions were relaxed in order to reach the values that correspond to energy minimum. The results are presented in Table 1.

It is clearly seen that our lattice constant results close to the experimental values with a small overestimation while an underestimation of bulk modulus is observed, that can be attributed to the general trend of PBE-GGA method which usually overestimates the lattice constant. The bulk modulus (B_0) is a measure of how resistant to compressibility that substance is, thus a large value of B_0 indicates high crystal rigidity.

2. Electronic Properties

To determine the nature of the electronic band structure, we calculated the density of states (DOS) of TiS_2. Thus, figure 2 shows the total and partial density of states obtained by mBJ-GGA for TiS_2.

From total DOS in Figure 2(a), we can distinguish, in the valence band, two separate regions. The first region, the valence lowest energy is due to S s-orbitals as is indicated in figure 2 (b). The second region is separated from the first by 6.7 eV. It is dominated by the Ti d and S-p orbitals in the figure 2(b). Lowest conduction region located above the Fermi level is formed mainly of states d of Ti atom with low contribution of states p of S atom. The second conduction region is separated from the first by 2.4 eV. It is dominated by the Ti-d states and S-p. The existence of a very strong hybridization between the d states of Ti and p states of S is also observed below the Fermi energy in the region from -5 to 0 eV.

The band structure of TiS_2 was calculated with theoretical lattice parameters obtained in the previous section. This gait makes sense in the context of a self-consistent first principle calculation and allows to compare the theoretical results at experience. The electronic band structure calculated along the lines of symmetry of the Brillouin zone (Figure 3) is presented in Figure 4. Like for all semiconductors, they are characterized by a band gap between the conduction band and the valence band. The minimum of the conduction band is located at L point and the maximum of the valence band is located at Γ point of the first Brillouin zone. This permits us to conclude that TiS_2 is a semiconductor with indirect gap equal to 0.26 eV, which is not far of the experimental value of 0.3 eV.[8]

3. Optical Properties

In this part, we will present some optical properties like dielectric function, refractive index, reflectivity, optical conductivity and absorption because those calculations play a vital role in the profound understanding of the nature of the material. All these properties can be calculated from the complex dielectric function:

$$\varepsilon(\omega) = \varepsilon_1(\omega) + i\,\varepsilon_2(\omega) \qquad (4)$$

where $\varepsilon_1(\omega)$ and $\varepsilon_2(\omega)$ are respectively the real and the imaginary parts of the dielectric function.

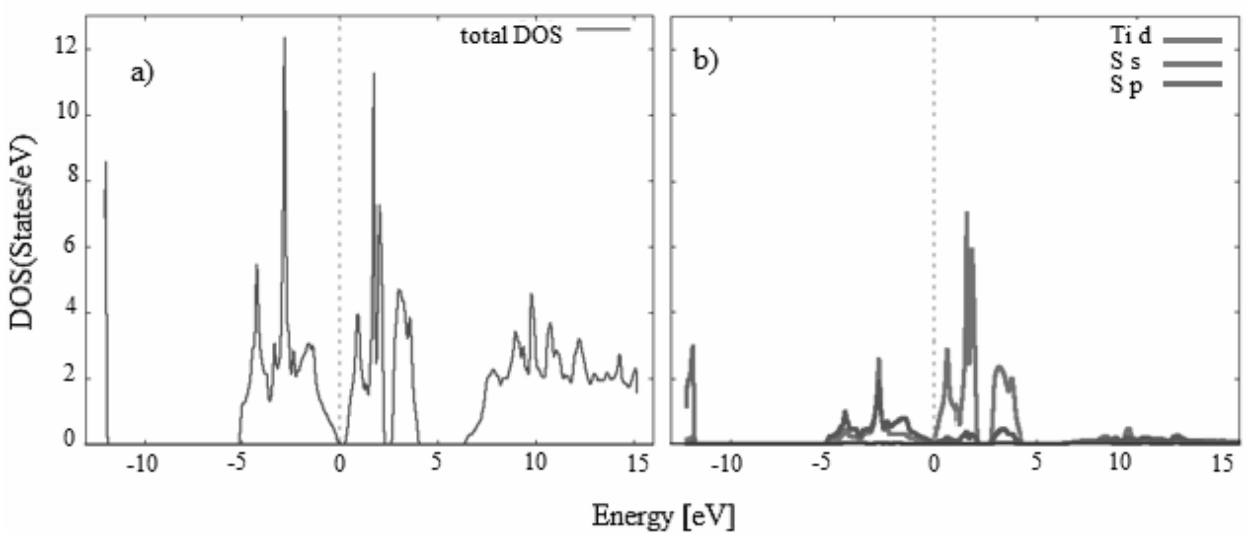

Fig. 2 – (a) Total and (b) Partial Density of state for TiS_2 within mBJ-GGA.

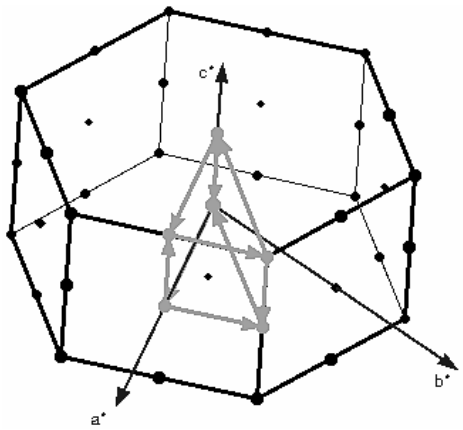

Fig. 3 – Brillouin zone and high-symmetry points for TiS_2.

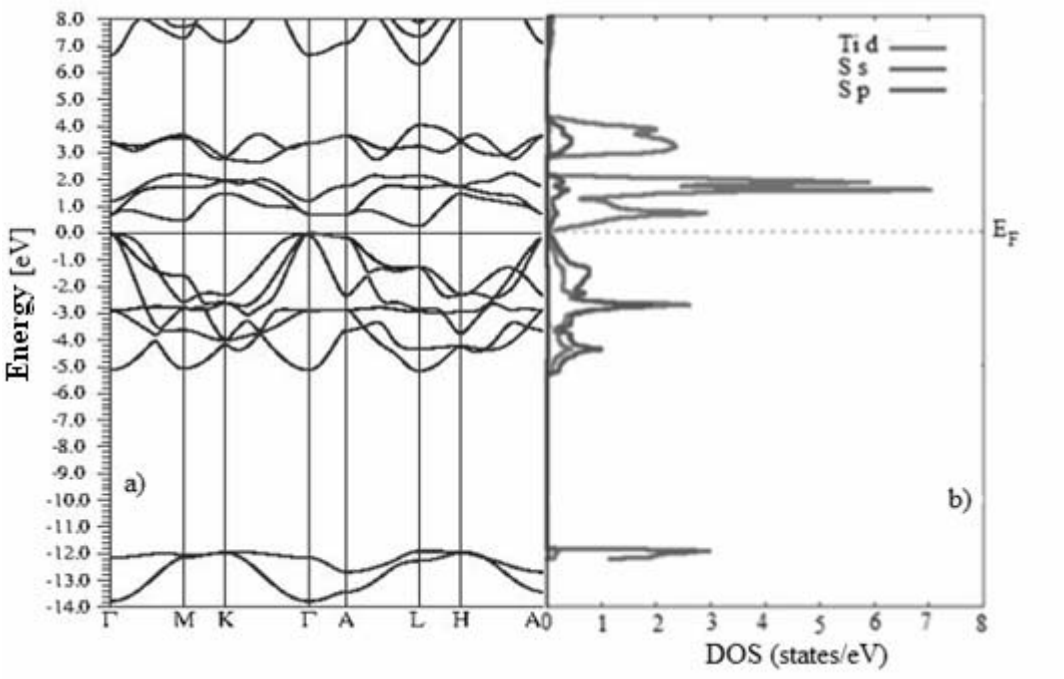

Fig. 4 – (a) Electronic band structures and (b) Partial electronic density of states of TiS_2.

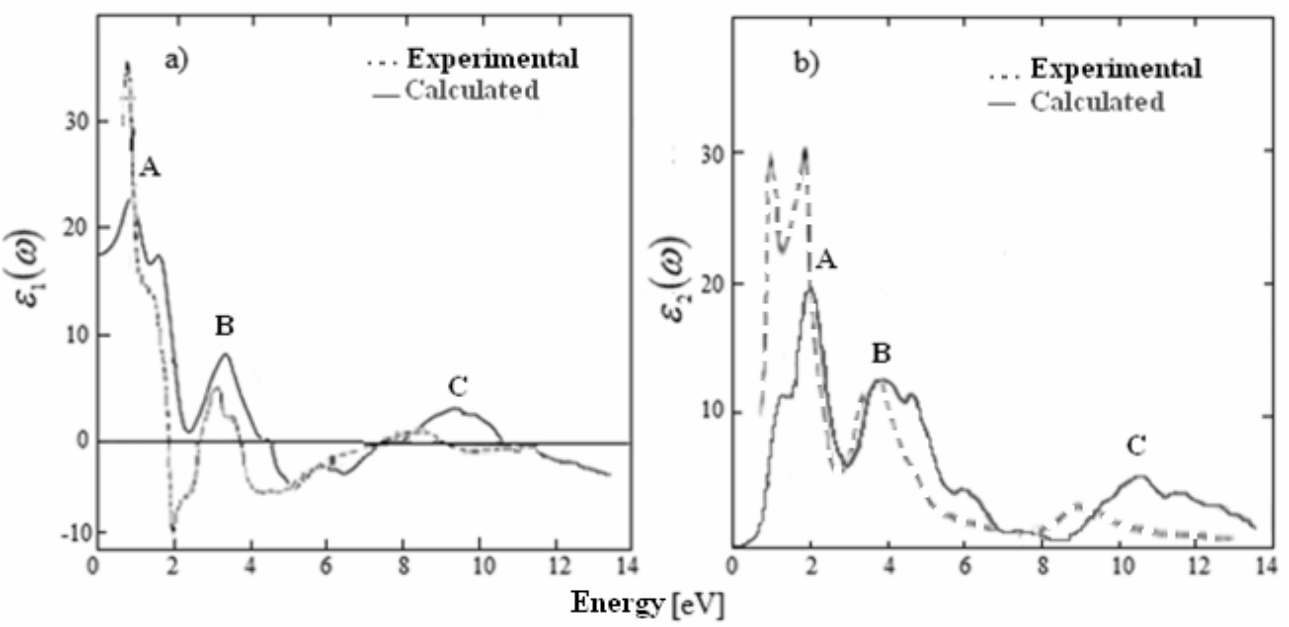

Fig. 5 – (a) Real part of dielectric function $\varepsilon_1(\omega)$, (b) Imaginary part of dielectric function $\varepsilon_2(\omega)$. Experimental values are dashed.[19]

This function allows describing the linear response of the system to excitation by an incident electromagnetic radiation.

In figures 5(a) and 5(b), we compare the curves obtained by calculation and experimentally, of respectively the real and imaginary parts of the dielectric function as a function of the energy of photon for TiS_2.

The real part of the dielectric function $\varepsilon_1(\omega)$ gives us information about the electronic polarizability of the material. The imaginary part $\varepsilon_2(\omega)$ is directly associated to the electronic band structure, and this last can be calculated by adding all possible occupied states to the unoccupied states of transitions.

The static dielectric constant at zero is $\varepsilon_1(0) = 17.5$, but the experimental value is equal to 30. From its zero frequency, the real part of the dielectric function $\varepsilon_1(\omega)$ increases in function of the energy and at 0.8 eV reaches the maximum value of 22.6 for calculated curve and 35.1 for the experimental. After, there is a dip in the amplitude of the real part of dielectric function and it attains a minimum negative value at 2 eV for experimental curve and at 2.2 eV for that calculated indicating that there is plasmonic excitation near 2 eV. Also, dip in $\varepsilon_1(\omega)$ at around 4.5 for experimental curve and at around 5.1 for that calculated indicate plasmon excitation.

The figure 5b shows calculated and experimental plot of imaginary part $\varepsilon_2(\omega)$ of the dielectric function for TiS_2. From those curves, we can distinguish 3 peaks: (A) at around 1.9 eV, for both experimental and calculated curves, (B) at around 4 eV, for both experimental and calculated curves and (C) at around 9 eV for experimental curve and at around 10.5 for that calculated. The imaginary part $\varepsilon_2(\omega)$ of the dielectric function is related to the absorption spectrum due to the electronic transitions from the valence band to conduction band. By comparing the peaks which appear in figure 5(b) with the figure 2 of the DOS, it is possible to deduce between which orbitals these transitions are made. Thus, it can be recognized that the peaks A, B and C in figure 5(b) are mainly due to transitions from S-p valence bands to Ti-d conduction bands. At a higher energy, the spectrum is without structures and decays very rapidly as function of the energy of photon.

The optical reflectivity is one of the most important parameters in optical calculations. In fact, reflectivity is responsive to a complicated combination of $\varepsilon_1(\omega)$ and $\varepsilon_2(\omega)$. This is generally described by the portion of the light energy reflected from the material surface. In figure 6(a), we have displayed the frequency dependent reflectivity $R(\omega)$.

Calculated and experimental reflectivity spectra of TiS_2 consist of three main, strong bands with several fine structures superimposed. The first two

bands, centered at about 2 eV and 5 eV, are approximately 2 and 3 eV wide. The third one having a better shape in experimental curve is centered at about 10.8 eV and is also approximately 3 eV wide. Our calculated spectra differ from experimental ones essentially for the relative intensities of the peaks, in the interval 0.6 - 12 eV.

Figure 6 (b) shows the calculated absorption coefficient as a function of the frequency using mBJ-GGA method. Similar features are observed in absorption coefficient in the absorption range up to 14 eV, it also shows three structures as in $\varepsilon_1(\omega)$, $\varepsilon_2(\omega)$ and *R(ω)*.

The optical conductivity as function of frequency for TiS_2 calculated with mBJ-GGA is shown in the figure 7(a). His behavior follows that of the imaginary part of the dielectric function $\varepsilon_2(\omega)$, since those two quantities are proportional.

The energy loss function *L(ω)* calculated with mBJ-GGA is displayed in Figure 7(b). This function *L(ω)* is an important factor describing the energy loss during the fast electron traversing in a material. The peaks in *L(ω)* spectra represent the characteristic associated with the plasma resonance. The resonant energy loss is seen at about 8 eV.

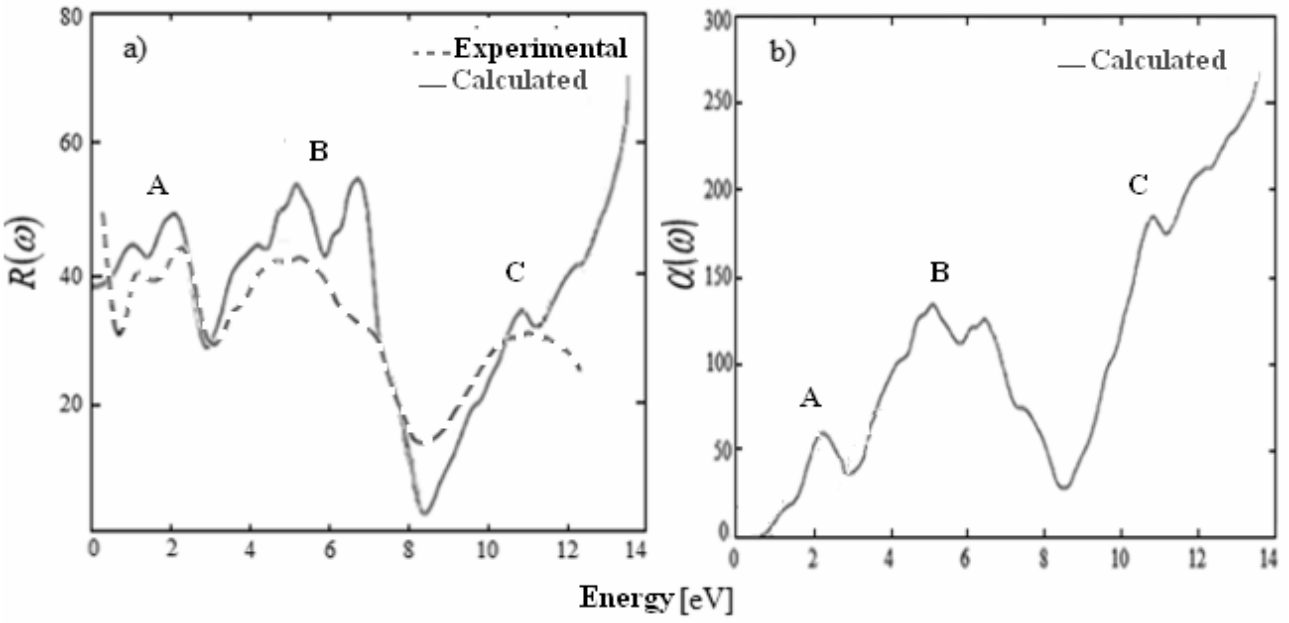

Fig. 6 – (a) Reflectivity spectrum *R(ω)*, (b) Absorption coefficient *α(ω)*. Experimental values are dashed.[20]

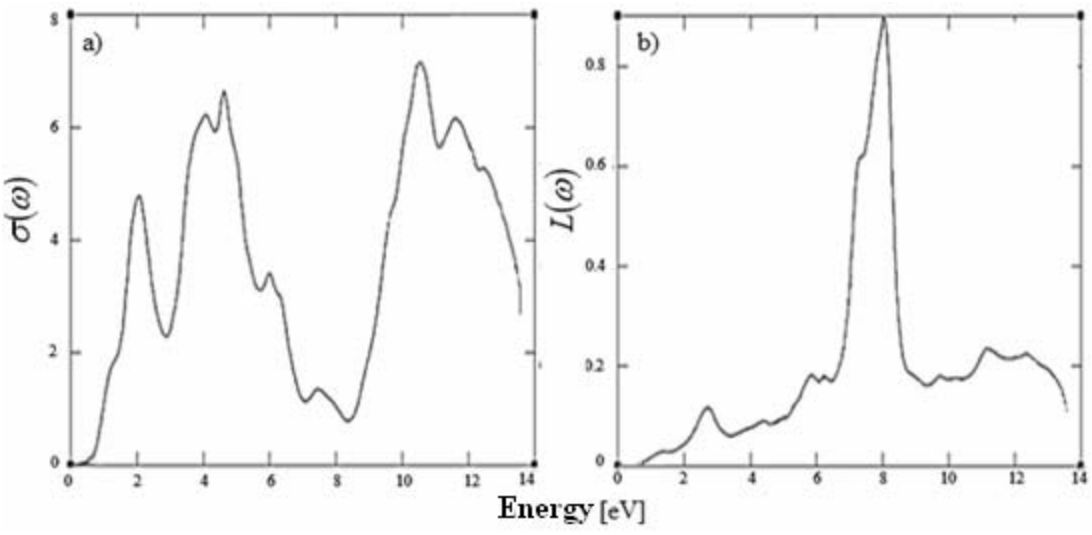

Fig. 7 – Frequency dependent (a) Optical conductivity σ(ω) (b) Energy-loss spectrum *L(ω)*.

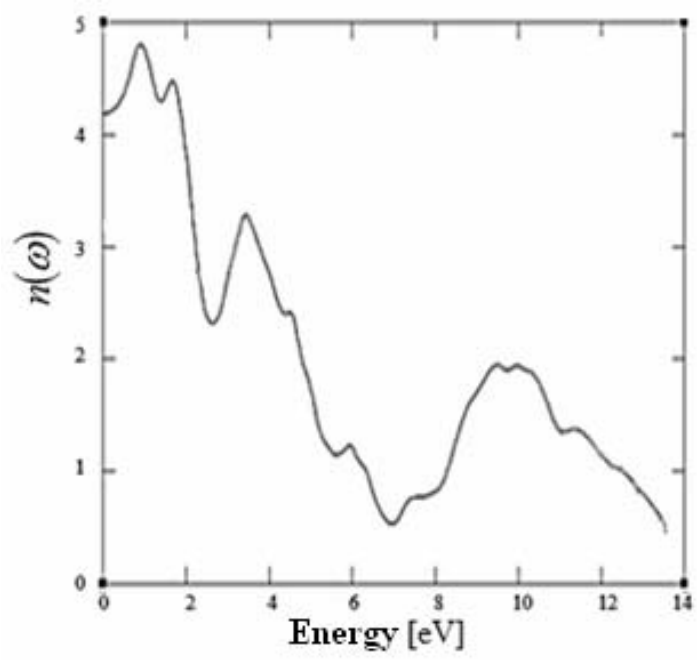

Fig. 8 – Refractive index *n(ω)* of TiS_2 within mBJ-GGA.

The calculated refractive index *n(ω)* for TiS_2 compound in range of energy (0 –14 eV) is depicted in Figure 8. We observe the optically anisotropic nature of this compound. The refractive index spectrum *n(ω)* follows the real part of the dielectric function $\varepsilon_1(\omega)$ because it is closely linked to this latter. The calculated refractive index at zero frequency for TiS_2 is found to be equal approximately to 4.2. The refractive index *n(ω)* spectrum of TiS_2 shows two significant features. First, a maximum is observed in the spectrum at about 0.9 eV, in infrared range. When the refractive index is greater than one, photons entering in material are slowed down by their interactions with electrons. The more photons are slowed down while travelling through the material, the greater is the refractive index. Generally, any mechanism that increases electron density in a material also increases its refractive index. Secondly, the refractive index of TiS_2 goes below one, between 6.3 eV and 8.3 eV.

CONCLUSION

In this paper we investigated structural, electronic and optical properties of TiS_2, using DFT based FP-LAPW method with new technique known as modified Becke-Johnson potential (mBJ). We report for the first time, a much accurate study of electronic band structure and of the optical parameters of the compound. We have found that TiS_2 has a semiconductor character with indirect gap of about 0.26 eV, which is in very close agreement to the experimental result of 0.3 eV. The achieved structural properties, with an optimization using PBE-GGA, are in suitable agreement with other found theoretical and experimental works. We have calculated the frequency dependent dielectric functions and we found considerable anisotropy. The frequency dependent dielectric functions show three main structures arising primarily from band transitions from the chalcogen p valence states to the Ti-d conduction states. We have also calculated the frequency dependent reflectivity and the absorption coefficient. Calculated static dielectric constant static refractive index and coefficient of reflectivity at zero frequency for TiS_2 within mBJ-GGA are also presented.

REFERENCES

1. M. Chhowalla, H. S. Shin, G. Eda, L .J. Li, K. P. Loh and H. Zhang, *Nat. Chem.*, **2013**, *5*, 263.
2. X. Su, R. Zhang, C. Guo, J. Zheng and Z. Ren, *Phys. Lett. A*, **2014**, *378*, 745.
3. K. Dolui and S. Sanvito, *EPL*, **2016**, *115*, 47001.
4. F. Yu, J. X. Sun and Y. H. Zhou, *Sol. Sta. Scie.*, **2012**, *12*, 1786.
5. A. L. Let, D. Mainwaing, C. Rix and P. Murugaraj, *Rev. Roum. Chim.*, **2007**, *52*, 235.
6. D. E. Mainwaring, A. L. Let, C. Rix and P. Murugaraj, *Sol. Sta.Comm.*, **2006**, *140*, 355.

7. Z. Zhu, Y. Cheng and U. Schwingenschlögl, *Phys. Rev. Lett.*, **2013**, *110*, 077202.
8. Q. Yan-Bin, Z. Guo-Hua, L. Di, W. Jiang-Lang, Q. Xiao-Ying and Z. Zhi, *Chin. Phys. Lett.*, **2007**, *24*,1050.
9. M. R. Ryzhikov, V. A. Slepkov, S. G. Kozlova, S. P. Gabuda and V. E. Fedorov, *Comp. and Theo. Chem.*, **2014**, *1027*,125.
10. D. Li, X. Y. Qin and Y. Gu, *Mat. Res. Bull.*, **2006**, *41*, 282.
11. H. El-Kouch, L. El Farh, J. Sayah and A. Challioui, *Chin. Phys. Lett.*, **2015**, *32*, 096102.
12. S. N. Li, J. B. Liu and B. X. Liu, *J. of Pow. Sour.*, **2016**, *320*, 322.
13. W. Kohn and L. S. Sham, *Phys. Rev. B*, **1965**, *140*, A 1133.
14. P. Blaha, K. Schwarz, G. Madsen, D. Kvasnicka and J. Luitz, WIEN2k, An Augmented Plane Wave + Local Orbitals Program for Calculating Crystal Properties; Karlheinz Schwarz, Techn. Univ. Wien: Austria, **2001**.
15. H. Martinez, Y. Tison, I. Baraille, M. Loudet and D. Gonbeau, *J. of Elec. Spect. and Rela. Phen.*, **2002**, *125*, 181.
16. F. Tran and P. Blaha, *Phys. Rev. Lett.*, **2009**, *102*, 226401(1).
17. A. D. Becke and M. R. Roussel, *Phys. Rev. A*, **1989**, *39*, 3761.
18. C. M. Fang, R. A. De Groot and C. Haas, *Phys. Rev. B*, **1997**, *56*, 8.
19. S. C. Bayliss and W. Y. Liang, *J. Phys. C*, **1985**, *18*, 3327.
20. D. L. Greenway and R. T. Nitsche, *Phys. Chem. Solids*, **1965**, *26*, 1445.